Al/γ-Al2O3 Interface in Laser Coated Aluminium Alloys

Zhou, X.B.; Hosson, J.Th.M. De

Published in:
Scripta Metallurgica et Materialia

DOI:
10.1016/0956-716X(95)00372-3

Publication date:
1995

Pergamon

Scripta Metallurgica *et* Materialia, Vol. 33, No. 8, pp. 1345-1351, 1995
Elsevier Science Ltd

0956-716X/95 $9.50 + .00

0956-716X(95)00372-X

Al/γ-Al_2O_3 INTERFACE IN LASER COATED ALUMINIUM ALLOYS

X. B. Zhou and J. Th. M. De Hosson
Department of Applied Physics, Material Science Centre,
University of Groningen,
Nijenborgh 4, 9747 AG Groningen, The Netherlands

(Received April 28, 1995)
(Revised June 22, 1995)

Introduction

Laser coating with a hard layer on top of aluminium alloys may significantly improve the wear resistance. However the selection of a particular coating material on aluminium alloys is rather subtle. For instance the solubility of metals in aluminium is sometimes limited [1], e.g. a homogeneous layer of Ni, Mn and Co could not be formed by laser processing [2]. In addition, as the wetting of aluminium on Al_2O_3 is poor, a well bonded layer of Al_2O_3 could be hardly formed [3]. The large differences of melting points and thermal expansion coefficients between Al_2O_3 and Al are also troublesome in the coating processing. In order to overcome these drawbacks, we have developed a laser coating process by means of a chemical reaction, where a reactive powder of SiO_2 [3] or Cr_2O_3 [4] has been applied on the surface of aluminium alloys. A layer of reaction product Al_2O_3 with 100 μm in thickness has been formed on aluminium alloys. Here we report a coating using Cr_2O_3 powders. According to the X-ray diffraction and energy dispersive spectrometry (EDS) results in the following exothermic chemical reaction takes place $Cr_2O_3 + Al = Al_2O_3 + Cr$ during the laser coating. Assuming that the reaction is processed at 900°C, then the free energy and the exothermic heat of the reaction can be calculated as -455 kJ/mole and 538 kJ/mole, respectively [4]. As it was pointed out earlier these negative free energy and exothermic heat are essential to the formation of a thick and well bonded coating on aluminium alloys [3][4].

It is known that the interface structure may affect the interface properties, e.g. wetting and bonding, and consequently the quality of the coating in practical applications. Therefore, here we concentrate on the interface structure that has been studied by transmission electron microscopy (TEM) and high resolution transmission electron microscopy (HREM).

Experiments

The materials to be coated are pure aluminium and commercial alloy Al6061 (1.0 wt% Mg, 0.6 wt% Si, 0.25 wt% Cu and 0.25 wt% Cr). Mixing powders of Cr_2O_3 and pure aluminium were used to coat both Al and Al6061. The size distribution of Cr_2O_3 powder ranges from 5 to 45 μm, and that of Al peaked around 60 μm.

A CW-CO_2 laser (Spectra Physics 820) was operated with an output power of 800 and 1200 W. The laser beam was defocused 20 mm and a beam diameter of 3 mm was obtained. A trace overlap of 67% was applied

Figure 1. TEM micrograph of an α-Al_2O_3 grain of a laser coating on Al6061.

in order to develop a sufficient thick layer. The scan velocity of the beam was 16 mm/s. The substrate was water cooled to prevent bulk melting during laser treatment. The coating process was employed by a home-made powder feeding system under Ar shielding atmosphere.

A JEM-200CX transmission electron microscope operating at 200 kV was used to study the microstructure and interfaces. Further, a high resolution transmission electron microscope (JEM-4000EX/II) with a point-to-point resolution of 0.17 nm resolution operating at 400 kV was employed. Simulation of HREM images was carried out using the EMS program [10] to compare the experimental images and the simulation images, In the simulation, an aperture diameter of 16 nm^{-1}, a spherical- aberration constant of C_s=1.0 mm, a spread of focus of δ=11 nm and a beam semi-convergence α_g=0.7 mrad were used. The specimen for both TEM and HREM were first cross sectioned and then glued together. Afterwards, the specimens were ground to about 200 μm and then mechanically dimpled down to 20 μm in the center. Ion milling was used for the final thinning.

Experimental Results

Fig.1 shows a TEM dark field image of the Cr_2O_3 coating on Al6061 which exhibits many small spherical Cr particles in the α-Al_2O_3 grain. The Cr particles are not coherent with the α-Al_2O_3 grains. Some of the Cr

Figure 2. TEM bright field image shows twinning of a-Al_2O_3 andCr_2O_3 in solid solution.

Figure 3. TEM bright field image of Al/γ-Al_2O_3 interface in a coating on Al6061. The (111) plane of the γ-Al_2O_3 is faceted at the interface.

particles are partly de-bonded from the α-Al_2O_3 . In Fig.2 a TEM bright field image indicates twinning of α-Al_2O_3 and Cr_2O_3 solid solution.

Fig.3 is a TEM bright field image of Al/γ-Al_2O_3 interface in the coating on Al6061. The (111) plane of the γ-Al_2O_3 is faceted at the interface. Fig.4 is the TEM bright field image and the [110] diffraction pattern of faceted spinel crystal at the interface from the coating on Al6061. According to the EDS composition analysis, there are a few percentages of Mg content in the γ-Al_2O_3 crystals which came from the Al6061 substrate during laser coating. As the lattice constants from the $MgAl_2O_4$ spinel and γ-Al_2O_3 spinel are rather close to each other, it is difficult to distinguish between them from the diffraction patterns. Therefore the interface of a reaction coating on pure aluminium has been examined.

Fig.5 represents a TEM bright field image of the Al/γ-Al_2O_3 interface in the coating on pure aluminium. Fig.6 illustrates a HREM image of the faceted interface on (111) g-Al2O3 plane. Fig.7 represents a TEM image of a defective γ-Al_2O_3 grain in the coating on pure Al. The diffraction patterns from [110] and [111] of the γ-Al_2O_3 crystals show superlattice diffraction spots and double diffraction which are depicted in Fig.

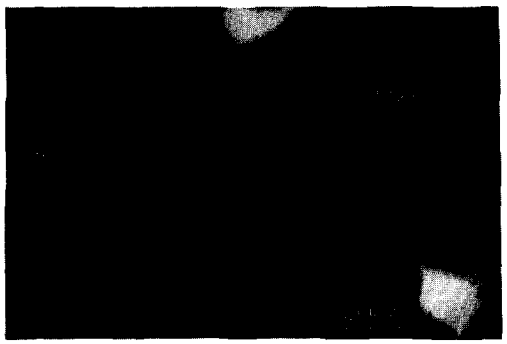

Figure 4. After a tilt of the TEM sample displayed in Fig.3, faceted γ-Al_2O_3 crystals at the interface can be seen along the [110] direction.

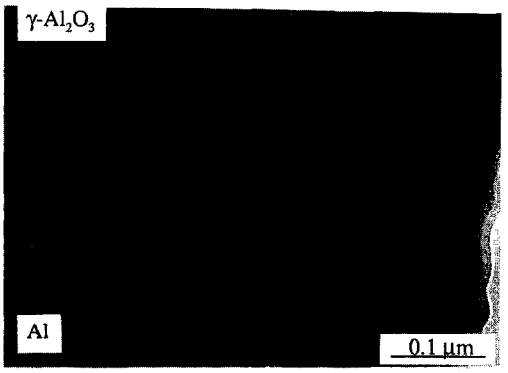

Figure 5. TEM bright field image of the interface in a coating on pure Al.

8. Fig.9 is a HREM image of γ-Al_2O_3 viewed along the [110] direction. A high density of stacking faults can be observed which cause the double diffraction.

Discussions

It is known that α-Al_2O_3 and Cr_2O_3 have the same hexagonal structure and the difference of the lattice constants between them are rather small, i.e. 4% to 4.4 %. As a result they form a complete solid solution in the whole range of composition [5]. A small amount of solid solution of Cr_2O_3 in Al_2O_3 may increase the hardness and especially may enhance the toughness of Al_2O_3 significantly. In contrast, γ-Al_2O_3 has a cubic spinel structure with the space group Fd3m and lattice constant of 0.790 nm [6]. It is a high temperature phase of Al_2O_3 which will slowly transform to α-Al_2O_3 at 1000°C [7]. Obviously γ-Al_2O_3 exists in the reaction layer due to the rapid cooling of the laser process.

It is interesting to discuss the effect of the γ-Al_2O_3 interface structure on the interface properties. It is known that the interface energy may have a substantial effect on the interface strength. Small lattice misfit of the interface, high density of structure defects and non-stoichiometric structure of the ceramic may alter the interface energy significantly. Suppose that γ-Al_2O_3 and Al is perfectly oriented at a {111} plane in the

Figure 6. HREM image of the faceted interface on a (111) γ-Al_2O_3 plane.

Figure 7. TEM image of a defective γ-Al_2O_3 grain in a coating on pure Al.

direction of <110>. Then, the lattice misfit of the interface is only around 2.5%, which is much smaller than that of 17.4% between γ-Al_2O_3 <100>{001} and Al <110>{111}. Consequently, the interface energy introduced by the lattice misfit is smaller for Al/γ-Al_2O_3 interface compared to that of Al/α-Al_2O_3 interface. Further, the distorted spinel structure of γ-Al_2O_3 points at more charged ions and defects in it, which may contribute to the interface stability due to charge induction and screening effects on the metallic side: i.e. it reduces the interface energy. Cao et al [8] reported that a γ-Al_2O_3 phase has been transformed from α-Al_2O_3 after a pulsed-laser irradiation. Pronounced lattice distortions existed in the re-solidified γ-Al_2O_3. They suggested that the rapid cooling rate after laser irradiation may prevent the ordering of Al atoms that is required for the formation of the stable α-Al_2O_3. Lowndes et al [9] have tested the bond strength of a copper film deposited onto a laser-treated α-Al_2O_3 surface. The bond strength is increased by a factor of 3 to 5

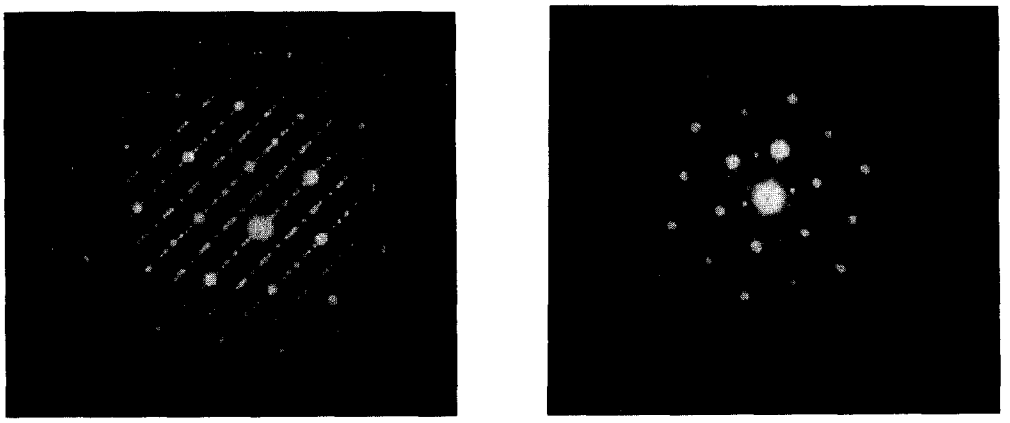

Figure 8. Diffraction patterns from [110] and [111] of the γ-Al_2O_3 which show superlattice diffraction spots and double diffraction.

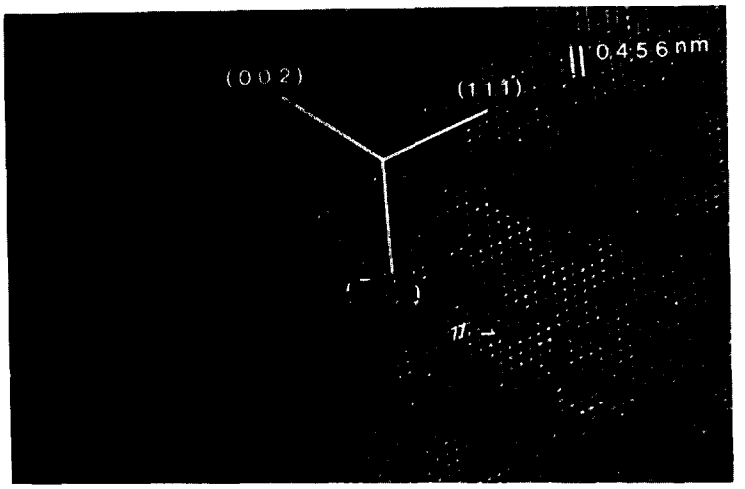

Figure 9. HREM image of γ-Al_2O_3 on [110]. High density stacking faults are seen.

compared to that of depositing a film onto a not laser-treated α-Al_2O_3 surface. Obviously the interface structure of γ-Al_2O_3 may be one of the principal reasons for an enhanced bond strength.

The HREM observation of high density stacking faults in the γ-Al_2O_3 crystals is consistent with the earlier work of the study of γ-Al_2O_3 stacking faults. According to the relative intensities of extra electron-diffraction spots to the normal spots, it was estimated that faults occurred at approximately one in every ten layers [10].

The small spherical Cr particles inside the α-Al_2O_3 are generated from the reaction between Cr_2O_3 and Al, where the Cr has no sufficient time to diffuse away. These Cr particles might absorb some thermal stresses of ceramic coating during rapid cooling and may help to prevent cracking.

Conclusions

It is shown that laser coating of aluminium alloys with Cr_2O_3 powder leads to the formation of α-Al_2O_3 and γ-Al_2O_3 . Many small Cr particles were found to be present inside the α-Al_2O_3 grains. In addition a high density of stacking faults in γ-Al_2O_3 grains was also been observed by HREM. The existence of the γ-Al_2O_3 at the metal-ceramic interface may improve the bond strength between the coating and the Al substrate.

Acknowledgements

This work is part of the research program of IOP-Metalen, The Hague, The Netherlands and of the Foundation for Fundamental Research on Matter (FOM-Utrecht) and has been made possible by financial support from the Netherlands Organisation for Research (NWO-The Hague)

References

1. H. J. Hegge, J. Boetje, J. Th. M. De Hosson, J. Mater. Sci., 25(1990), 2335
2. Alloy Phase Diagrams, ASM Handbook, Vol.3, P43,48 & 49
3. X. B. Zhou and J. Th. M. De Hosson, Scripta. Metal., 28(1993), 219
4. X. B. Zhou and J. Th. M. De Hosson, 94' International Conference on Laser Materials Processing, Chongqing, P. R. China, Oct.12-15, 1994.

5. E. M. Levin, C. R. Robbins and H. F. Mcmurdie, "Phase Diagrams for Ceramist", The American Ceramics Society, INC. (1964), 121(Fig.309)
6. J. E. Bonevich and L. D. Marks, J. Mater. Res., 7(1992), 1489
7. Powder Diffraction File JCPDS International centre, No. 10-425.
8. S. Cao, A. J. Pedraza, D. H. Lowndes and L. F. Allard, Appl. Phys. Lett. 65(1994), 2940
9. D. Lowndes M. Desilva, M. J. Godbole, A. J. Pedraza, T. Thundat and R. J. Warmack, Appl. Phys. Lett. 64(1994), 1791
10. J. M. Cowley, Acta Crystall., 6(1953), 53
11. A. Kochendorfer, Z. Kristallogr., A97(1938), 469; U. Dehlinger and A. Kochendorfer, Ibid., A101(1939), 13.
12. X. B. Zhou and J. Th. M. De Hosson, Acta Metall. Mater., 42(1994), 1155